Asian Journal of Chemistry; Vol. 29, No. 8 (2017), 1866-1870

ASIAN JOURNAL OF CHEMISTRY

https://doi.org/10.14233/ajchem.2017.20760

# Photoluminescence Studies of $ZnWO_4:Sm^{3+}$ Synthesized by Ethylene Glycol Route

N. PREMJIT SINGH[1,2], N. RAJMUHON SINGH[3] and N. MOHONDAS SINGH[1]

[1]Department of Chemistry, Mizoram University, Aizawl-796 004, India
[2]Department of Chemistry, A.R.S.D. College, University of Delhi, Dhaula Kuan, New Delhi-110 021, India
[3]Department of Chemistry, Manipur University, Canchipur-795 003, India

*Corresponding author: E-mail: nmdas08@rediffmail.com

*Received*: 5 May 2017; *Accepted*: 19 May 2017; *Published online*: 12 June 2017; AJC-18455

A series of crystalline $ZnWO_4$ doped $Sm^{3+}$ with different concentrations of dopant ion were successfully prepared by the co-precipitation method using ethylene glycol followed by annealing of the precipitates formed. The prepared sample was crystallized in monoclinic structure with spherical morphology and crystallite sizes extend in the ranges from 10-20 nm. Photoluminescence analysis of the samples showed that there exist strong absorption band with maximum around 275 nm and broad emission band due to $WO_6^{6-}$ group with maximum around 456 nm along with weakly intense peaks characteristics to the *f-f* transitions of $Sm^{3+}$ ion at 569, 612 and 653 nm. The optimum concentration of $Sm^{3+}$ ion in $ZnWO_4$ lattice is obtained at 3 at. % and beyond this, the emission intensity originated from $Sm^{3+}$ ion decreases due to concentration quenching.

**Keywords: $ZnWO_4:Sm^{3+}$, Photoluminescence, Concentration effect.**

## INTRODUCTION

In recent years, investigation on the rare earth activated inorganic phosphors has attracted to many researchers because of their potential applications in lighting and display devices including plasma display panels (PDPs), field emission displays (FEDs), light emitting diodes (LEDs), fluorescence lamp, cathode ray tubes and other optical devices *etc*. [1,2]. These materials consist of two components: one component being the host lattice and the other component being the activator ion, the rare earth doping ions behave as the activator ion [3]. Among the rare earth ions, $Sm^{3+}$ with $f^5$ configuration is very interesting ion because of its high quantum efficiency [4] and generally this ion emits in the orange region due to the transitions of $^4G_{5/2}$-$^6H_{J/2}$ ($J$ = 5/2, 7/2, 9/2 and 11/2) induced by efficient energy transfer from host lattice to $Sm^{3+}$ ion or by direct excitation process.

It is well known that zinc tungstate exhibits high thermal and chemical stability, non-hygroscopic and high average refractive index [5,6]. It is crystallized in monoclinic wolframite structure with each of $Zn^{2+}$ and $W^{6+}$ ions are surrounded by six O sites and formed distorted octahedral geometry of $ZnO_6$ and $WO_6$ [7]. It is very interesting and widely investigated compound due to its potential applications in scientillation [8, photocatalyst [9], photoluminescence [6,8] and sensors [10,11] *etc*. Since $ZnWO_4$ is widely used scintillating crystal, the luminescence property of this material is largely investi-gated and it has been reported that the intrinsic luminescence is arise from the charge transfer transition within the $WO_6^{6-}$ complex [8,12-14]. However, till now, there have been only few papers reported on the synthesis and photoluminescence studies of $RE^{3+}$ activated $ZnWO_4$ lattice. For example, Liao *et al.* [13] reported synthesis and photoluminescence properties of $ZnWO_4:Tb^{3+}$ co-doped with different charge compensators. White color emission of $Eu^{3+}$ and $Dy^{3+}$ co-doped $ZnWO_4$was reported by Zhai *et al.* [14]. Dai *et al.* [6] investigated the effect of surface defect and pH of the solution on the photoluminescence properties of $ZnWO_4:Eu^{3+}$. He [15] reported the synthesis and photoluminescence property of $Sm^{3+}$ doped $ZnWO_4$ powders and films with wet chemical methods. Ran *et al.* [5] reported fabrication of $ZnWO_4:Sm^{3+}$, $Bi^{3+}$, $Li^+$ with tunable white light emitting properties for W-LEDs application. Zhai and his co-workers [16] investigated white light emission properties of $ZnWO_4:Dy^{3+}$ synthesized by hydrothermal process. It is found from the observations of previous studies that more investigations of $RE^{3+}$ activated $ZnWO_4$ are essential. Therefore in the present investigation, we have synthesized $ZnWO_4:Sm^{3+}$ by using ethylene glycol (EG) as capping agent as well as reaction medium. The luminescence properties of the phosphors with different concentrations of the dopant $Sm^{3+}$ ion were also investigated. To the best of our knowledge, the synthesis of $ZnWO_4:Sm^{3+}$ by ethylene glycol route and

studies of its photoluminescence properties have not been reported yet.

## EXPERIMENTAL

**Sample preparation:** In this work, $ZnWO_4:Sm^{3+}$ (1, 2, 3, 5 and 7 at. %) crystals were prepared by co-precipitation method using ethylene glycol as reaction medium as well as capping agent. The chemicals used were $ZnCl_2$ (AR) (98 %) from Thomas baker, $Na_2WO_4$ (98 %) from Himedia and $SmCl_3·H_2O$ (99.9 %) from Alpha Aesar. In a typical synthesis, stoichiometric amounts of $ZnCl_2$ and $SmCl_3$ were taken in a round bottom flask. After that, the mixture was dissolved in 30 mL of ethylene glycol. $Na_2WO_4$ solution separately dissolved in 30 mL of ethylene glycol was then added to the above solution and then, the solution was refluxed at 180 °C for 3 h. The precipitate thus formed was centrifuged and washed with double distilled water for about 4-5 times and finally with acetone. The observed white precipitate was dried in an oven at a temperature of about 50-70 °C for 12 h and then annealed at 500 °C for 3 h.

**Characterization:** The phase composition and crystal structure of the prepared sample was determine by the X-ray diffraction (XRD) using PANalytical powder diffractometer with $CuK_\alpha$ (1.5406 Å) radiation and Ni filter. The vibrational spectra of the samples were recorded by Perkin Elmer Fourier transform infrared (FT-IR) spectrometer RXI using KBr as beam splitter in the ranges between 4000-400. JEOL transmission electron microscope (TEM) JEM-2100 was used for the measurements of TEM image, high resolution transmission electron microscope (HRTEM) image and selected area electron diffraction (SAED) pattern. Energy dispersive analysis of X-rays (EDAX) spectrum was recorded using FEI quanta 250. The excitation and emission spectra of the prepared samples were recorded using F-7000 Hitachi fluorescence spectrophotometer with xenon discharge lamp as the excitation source. All the measurements were taken at room temperature.

## RESULTS AND DISCUSSION

**X-ray diffraction analysis:** In order to find the crystal structure and phase composition, the prepared $ZnWO_4:Sm^{3+}$ (3 at. %) was subjected to X-ray diffraction. Fig. 1 shows the XRD pattern and on comparing the relative intensities and *d*-space values of the peaks, the observed peaks are well matched with the monoclinic structure of $ZnWO_4$ with lattice constants of, a = 4.691; b = 5.720; c = 4.925 and lattice volume V = 132.14 $Å^3$ and space group of P2/C (JCPDS card number 15-0774). Further, no peaks due to starting materials such as $SmCl_3$ and other impurities were detected, which indicates that the dopant $Sm^{3+}$ ions have been doped into the lattice. The rough crystallite size of the sample calculated from the broadening of the most intense peak (111) by using Scheers equation $D = 0.9\lambda/\beta \cos\theta$ is 14.5 nm. Here, D represents crystallite diameter; λ is wavelength of the X-ray used (1.546) and β denotes full width half maximum and θ is an angle of diffraction in radian.

**FT-IR analysis:** The vibrational modes of the prepared samples were investigated by the FT-IR spectrometer. Fig. 2 shows FT-IR spectra of $ZnWO_4:Sm^{3+}$ (1 and 3 at. %) and it is observed from the spectra that those peaks observed at around 3443 and 1634 $cm^{-1}$ are assigned to stretching and bending

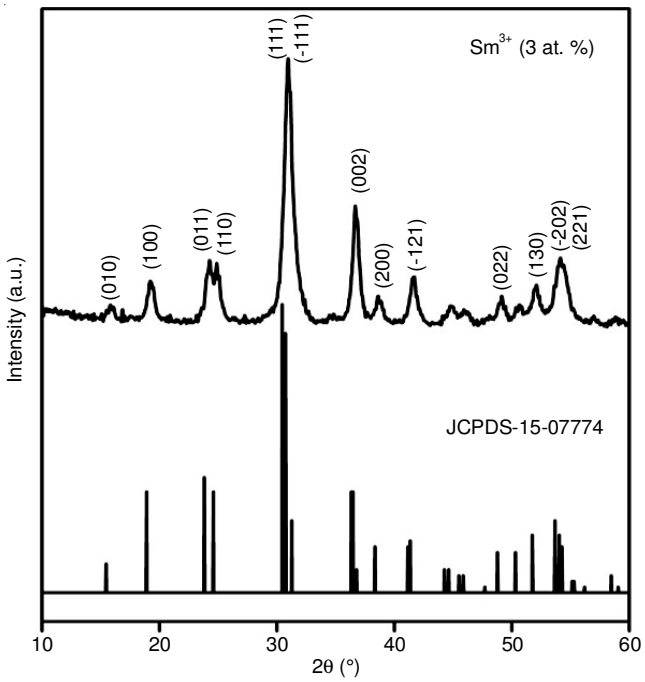


Fig. 1. XRD pattern of $ZnWO_4:Sm^{3+}$ (3 at. %)

vibrational modes of O-H bond respectively [9], which means that the prepared samples are hydroxylated. The peaks observed at about 877 and 833 $cm^{-1}$ are attributed to the stretching and bending vibrational modes of Zn-O-W bonds, respectively and the peaks exhibited around 697and 540 $cm^{-1}$ are assigned to the stretching and bending vibrational modes of W-O bond within the $WO_6^{6-}$ group, respectively while the observed peak around 460 $cm^{-1}$ is ascribed to the vibrational mode of Zn-O bond [17]. In addition, a peak with weakly intense was observed around 2975 $cm^{-1}$, which is attributed to the vibrational mode of $CH_2$-group originating from the ethylene glycol [18,19]. From the above results, it can be suggested that the prepared tungstate compound contained adsorbed $H_2O$ molecule and the ethylene glycol used in synthesis is not completely removed.

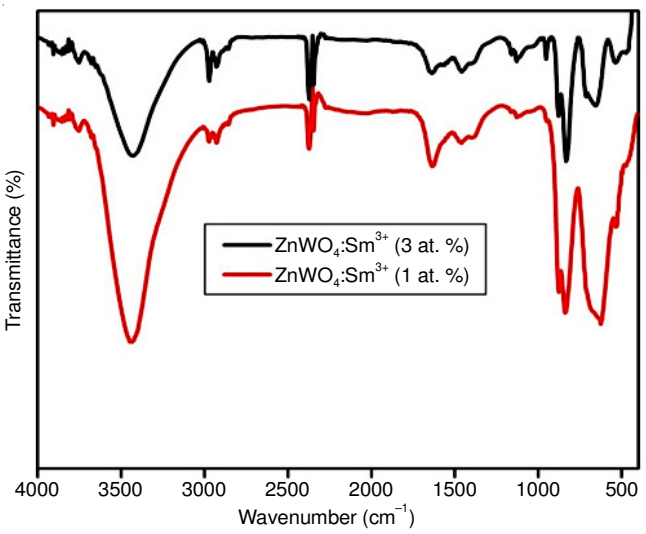


Fig. 2. FT-IR spectra of $ZnWO_4:Sm^{3+}$ (1 and 3 at. %)

**TEM analysis:** It is well known that the luminescence property of a phosphor is highly dependent on its morphology

and therefore, as far as luminescence of a phosphor is concerned, determination of morphology is very essential. So, in order to examine morphology, $ZnWO_4:Sm^{3+}$ (3 at. %) was subjected to TEM and the obtained image is shown in Fig. 3a. It is revealed from the image that the sample is crystallized with spherical morphology and crystallites diameter extends in the ranges from 10 to 20 nm, which is in close agreement with the size calculated from XRD data. From the observed inter planar lattice fringes in high resolution transmission electron microscope (HRTEM) image (Fig. 3b) and circular dotted rings in selected area electron diffraction (SAED) pattern (Fig. 3c), it is evident that the prepared sample formed polycrystalline with high crystallinity. Fig. 3d shows EDAX spectra, which is very important for elemental analysis and the observed spectra contained peaks due to Zn, O, W and Sm. Entering of $Sm^{3+}$ into the $ZnWO_4$ lattice is further supported by this result.

**Photoluminescence analysis:** The excitation spectra of $ZnWO_4:Sm^{3+}$ monitoring emission wavelength at 610 nm is shown in Fig. 4. It consists of a broad and strong band in the ranges from 230 to 310 nm with maximum around 275 nm. This band can be attributed to the charge transfer transition from the filled 2*p* orbital of oxygen to the empty 5*d* orbital of $W^{6+}$ within the $WO_6^{6-}$ complex [13,15]. In addition, it is also observed in the spectra some irregularities in the form of zig-zag at the longer wavelength region especially after 400 nm.

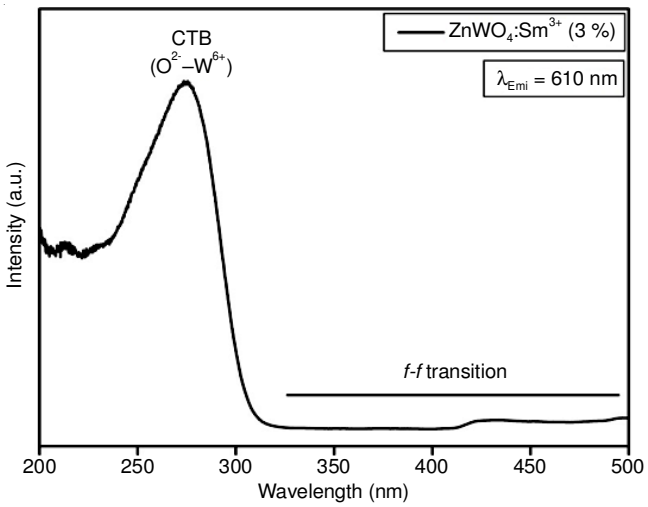


Fig. 4. Excitation spectra of $ZnWO_4:Sm^{3+}$ (3 at. %)

It is suggested that this irregularities are induced due to the *f-f* transitions of dopant $Sm^{3+}$ ions and these peaks were not identified clearly due to they are weakly intense as compare to the strong broad band of $O^{2-}$-$W^{6+}$ transition. Fig. 5a shows emission spectra of $ZnWO_4:Sm^{3+}$ with different concentrations of $Sm^{3+}$ ions doping and it consists of a broad and strong band in the range from 407 to 579 nm with maximum intensity around

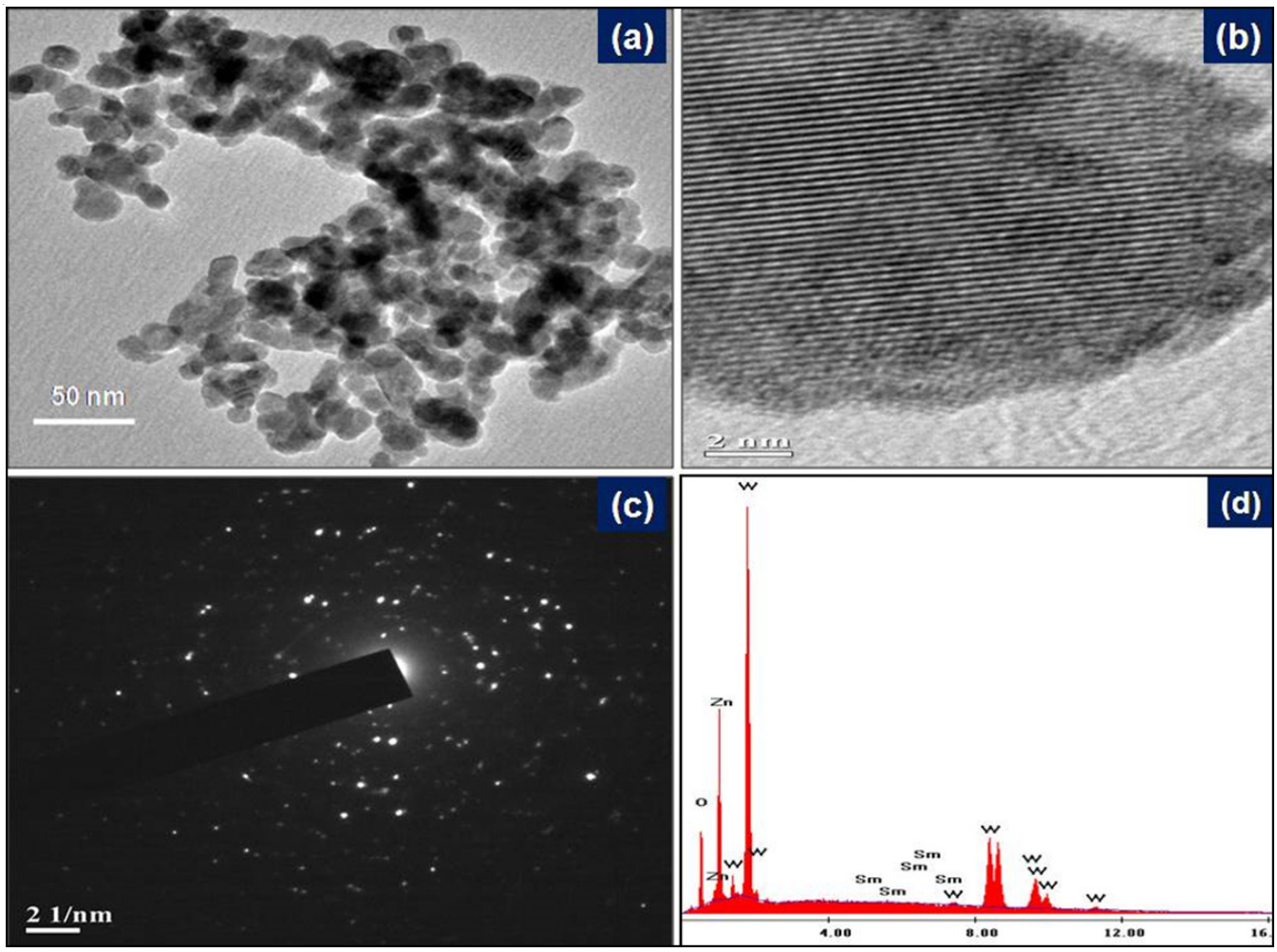


Fig. 3. (a) TEM image, (b) HRTEM image, (c) SAED pattern and (d) EDAX spectra of $ZnWO_4:Sm^{3+}$ (3 at. %)

456 nm. It is believed that this broad band is induced by the $WO_6^{6-}$ complex and slight deviation from perfect crystal structure and its luminescence properties are determined by the charge transfer transition from excited 2*p* orbitals of oxygen to the empty 5*d* orbitals of tungsten ion [6]. Further, it is clearly seen from the spectra that the intensity of the broad band emission is highly dependent on the concentrations of $Sm^{3+}$ ion, the intensity increases with the increase of $Sm^{3+}$ ion contents. In addition to this, the spectra exhibited series of sharp peaks characteristics to the *f-f* transitions of $Sm^{3+}$ ion centering at 569, 612 and 653 nm and they are assigned to the $^4G_{5/2}$-$^6H_{5/2}$, $^4G_{5/2}$-$^6H_{7/2}$ and $^4G_{5/2}$-$^6H_{9/2}$ transitions, respectively [20,21]. Fig. 5b shows the enlarged emission spectra in the wavelength ranges from 560 to 740 nm and the inset in the figure shows the emission peak observed at 715 nm due to $^4G_{5/2}$-$^6H_{11/2}$ transition of $Sm^{3+}$. It is well known that the integrated area under the peak represents the intensity of the peak and therefore we have calculated the integrated areas of $^4G_{5/2}$-$^6H_{7/2}$ and $^4G_{5/2}$-$^6H_{9/2}$ transitions in the wavelength range between 600-620 and 635-670 nm, respectively in order to examine the effect of $Sm^{3+}$ ion concentration on the photoluminescence intensities for the peaks originated from the dopant $Sm^{3+}$ ion and they are given in Table-1. From the table, it is revealed that there is no significant change in the peak position and full width half maximum values with the change of $Sm^{3+}$ ions contents, indicating no change in the site symmetry around $Sm^{3+}$ ions; but the values of integrated area are considerably changing. Fig. 5c shows a plot of integrated intensity with respect to concentration of $Sm^{3+}$ contents and it is revealed from the figure that the integrated intensity increases with the increase of $Sm^{3+}$ ion and reached maximum at $Sm^{3+}$ (3 at. %); then, the integrated intensity decreases with further increase in the $Sm^{3+}$ ion concentration. So, the optimum concentration of $Sm^{3+}$ ion in this case is 3 at. % and the reduction in the integrated intensity after this particular concentration is due to the concentration quenching phenomenon of $Sm^{3+}$ ion. In this phenomenon, the interionic separation between the nearby $Sm^{3+}$ ions decreases at higher concentrations of $Sm^{3+}$ ions and therefore non-radiative energy transfer between the neighbouring $Sm^{3+}$ions took place, consequently the radiative emission decreases.

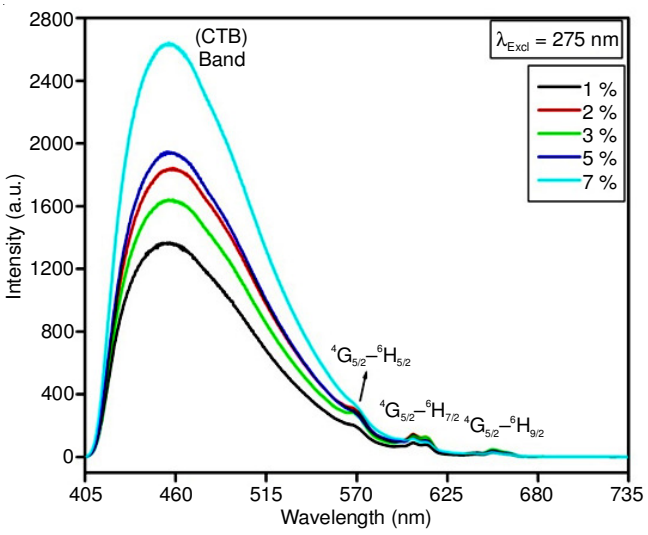


Fig. 5a. Emission spectra of $ZnWO_4$:$Sm^{3+}$

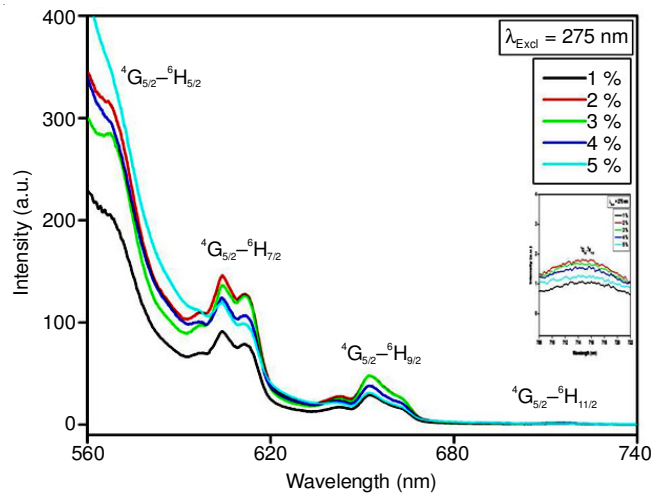


Fig. 5b. Enlarged emission spectra of $ZnWO_4$:$Sm^{3+}$ in the wavelength ranges from 560-740 nm

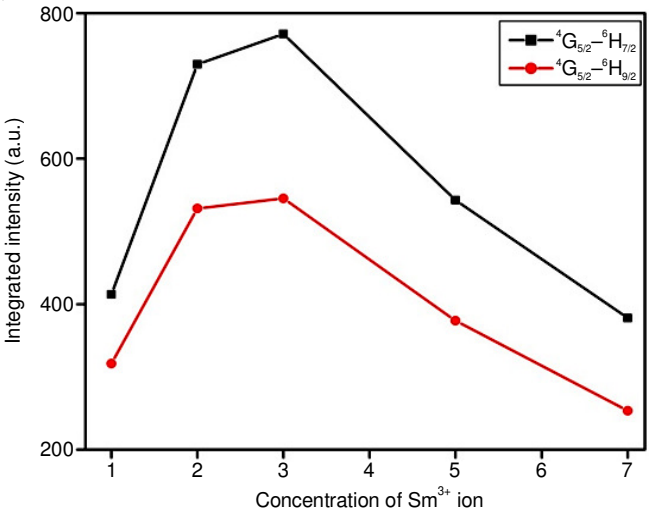


Fig. 5c. Plot of integrated intensity *vs.* concentrations of $Sm^{3+}$ ion

TABLE-1
VALUES OF INTEGRATED AREA ($A_1$ AND $A_2$), FULL WIDTH HALF MAXIMUM ($W_1$ AND $W_2$) AND PEAK POSITION OF $^4G_{5/2}$-$^6H_{7/2}$ AND $^4G_{5/2}$-$^6H_{9/2}$ TRANSITIONS FOR $ZnWO_4$:x$Sm^{3+}$ (x = 1, 2, 3, 5 and 7 at. %)

| $Sm^{3+}$ ion conc. (at. %) | $^4G_{5/2}$-$^6H_{7/2}$ (600-620 nm) | | | $^4G_{5/2}$-$^6H_{9/2}$ (635-670 nm) | | |
|---|---|---|---|---|---|---|
| | Integrated area ($A_1$) | Full width half maximum (FWHM) ($W_1$) | Peak position | Integrated area ($A_2$) | Full width half maximum (FWHM) ($W_2$) | Peak position |
| 1 | 413.26 | 13.6 | 613.2 | 318.46 | 14.2 | 653.0 |
| 2 | 729.86 | 13.6 | 612.8 | 531.51 | 14.2 | 652.2 |
| 3 | 771.37 | 13.4 | 612.6 | 545.36 | 14.2 | 652.6 |
| 5 | 543.16 | 13.6 | 612.2 | 377.14 | 14.0 | 652.2 |
| 7 | 381.02 | 13.8 | 612.2 | 253.49 | 13.2 | 652.2 |

## Conclusion

In conclusion, $ZnWO_4:Sm^{3+}$ nanocrystals were successfully prepared by the co-precipipitation method using ethylene glycol as capping agent followed by annealing of the precipitates formed. The spherical shape crystallites extended their sizes in the ranges from 10-20 nm. Analysis of the excitation and emission spectra resulted in the production of broad band due to charge transfer transition within the $WO_6^{6-}$ complex. It is also produced sharp and weakly intense emission peaks characteristics to the dopant $Sm^{3+}$ ions and the optimum concentration was observed at 3 at. %, after that due concentration quenching of $Sm^{3+}$ ion, the emission intensity decreases.

## ACKNOWLEDGEMENTS

The authors are very thankful to Sophisticated Analytical Instrument Facility (SAIF), North Eastern Hill University (NEHU), Shillong, India for providing TEM facility, University Science Instrumentation Center (USIC), University of Delhi, for providing FTIR facility and the Science and Engineering Research Board (SERB), New Delhi, India (Vide No. SB/EMEQ-336/2014 date 04.02.2016) for financial support.

## REFERENCES

1. S. Gai, C. Li, P. Yang and J. Lin, *Chem. Rev.*, **114**, 2343 (2014); https://doi.org/10.1021/cr4001594.
2. S. Ye, F. Xiao, Y. Pan, Y. Ma and Q. Zhang, *Mater. Sci. Eng. Rep.*, **71**, 1 (2010); https://doi.org/10.1016/j.mser.2010.07.001.
3. D. Wang, J. Fan, M. Shang, K. Li, Y. Zhang, H. Lian and J. Lin, *Opt. Mater.*, **51**, 162 (2016); https://doi.org/10.1016/j.optmat.2015.11.029.
4. M. Sobczyk and D. Szymanski, *J. Lumin.*, **142**, 96 (2013); https://doi.org/10.1016/j.jlumin.2013.03.062.
5. W.G. Ran, Q. Wang, Y.R. Zhou, S.T. Ding, J.S. Shi and J.H. Jeong, *Mater. Res. Bull.*, **64**, 146 (2015); https://doi.org/10.1016/j.materresbull.2014.12.050.
6. Q. Dai, H. Song, X. Bai, G. Pan, S. Lu, T. Wang, X. Ren and H. Zhao, *J. Phys. Chem. C*, **111**, 7586 (2007); https://doi.org/10.1021/jp066712e.
7. J. Arin, P. Dumrongrojthanath, O. Yayapao, A. Phuruangrat, S. Thongtem and T. Thongtem, *Superlatt. Microstruct.*, **67**, 197 (2014); https://doi.org/10.1016/j.spmi.2013.12.024.
8. T. Oi, K. Takagi and T. Fukazawa, *Appl. Phys. Lett.*, **36**, 278 (1980); https://doi.org/10.1063/1.91452.
9. R. Shi, Y. Wang, D. Li, J. Xu and Y. Zhu, *Appl. Catal. B*, **100**, 173 (2010); https://doi.org/10.1016/j.apcatb.2010.07.027.
10. L. You, Y. Cao, Y.F. Sun, P. Sun, T. Zhang, Y. Du and G.Y. Lu, *Sens. Actuators B Chem.*, **161**, 799 (2012); https://doi.org/10.1016/j.snb.2011.11.035.
11. X. Cao, W. Wu, N. Chen, Y. Peng and Y. Liu, *Sens. Actuators B Chem.*, **137**, 83 (2009); https://doi.org/10.1016/j.snb.2008.11.020.
12. H. Grassmann, H.-G. Moser and E. Lorenz, *J. Lumin.*, **33**, 109 (1985); https://doi.org/10.1016/0022-2313(85)90034-1.
13. J. Liao, D. Zhou, X. Qiu, Sh. Liu and H.-R. Wen, *Optik*, **124**, 5057 (2013); https://doi.org/10.1016/j.ijleo.2013.03.067.
14. Y. Zhai, M. Wang, Q. Zhao, J. Yu and X. Li, *J. Lumin.*, **172**, 161 (2016); https://doi.org/10.1016/j.jlumin.2015.11.037.
15. H.Y. He, *Phys. Status Solidii, B Basic Res.*, **246**, 177 (2009); https://doi.org/10.1002/pssb.200844218.
16. Y. Zhai, X. Li, J. Liu and M. Jiang, *J. Rare Earths*, **33**, 350 (2015); https://doi.org/10.1016/S1002-0721(14)60425-7.
17. P. Siriwong, T. Thongtem, A. Phuruangrat and S. Thongtem, *CrystEngComm*, **13**, 1564 (2011); https://doi.org/10.1039/C0CE00402B.
18. K.G. Sharma and N.R. Singh, *New J. Chem.*, **37**, 2784 (2013); https://doi.org/10.1039/c3nj00155e.
19. W. Kemp, Organic Spectroscopy, Macmillan, Hampshire, edn 3 (1975).
20. N.P. Singh, N.R. Singh and N.M. Singh, *Asian J. Chem.*, **28**, 2103 (2016); https://doi.org/10.14233/ajchem.2016.19996.
21. G. Blasse and B.C. Grabmaier, Luminescent Materials, Springer-Verlag, Berlin (1994).